Journal of Marine Research, 60, 835–854, 2002

Recent turbidite deposition in the eastern Atlantic: Early diagenesis and biotic recovery

by P. Anschutz[1], F. J. Jorissen[1,2], G. Chaillou[1], R. Abu-Zied[3] and C. Fontanier[1]

ABSTRACT

An interface core taken in Capbreton canyon shows a succession of sedimentary facies interpreted as classical Bouma turbiditic sequences. Activities of ^{234}Th and ^{210}Pb suggest that the deposition of the most recent turbidite was triggered by the violent storm that affected the Atlantic coast of southern France on the 27th of December 1999, about four months before the sampling of the core. This turbidite allows us to study the ongoing diagenesis of the new sediment layer and of the previous sediment-water interface, which has been buried and only slightly eroded. A study of benthic foraminiferal populations informs us about the rate of benthic ecosystem recovery after such a major ecosystem disturbance event. The composition of the benthic foraminiferal fauna suggests that the benthic ecosystem in Capbreton canyon remains in an early stage of colonization. The rare agglutinant taxon *Technitella melo* appears to be the first colonizing species. It is suggested that *Technitella melo* is advantaged by the food-impoverished conditions in the days following turbidite deposition. Almost all of the turbidite layer and the previous oxic sediment-water interface contain reduced dissolved metal species and were anoxic. The buried interface contains Fe- and Mn-oxides inherited from its recent oxic past. The reduction of manganese oxides was in progress at the time of core collection. The reduced Mn remained trapped in the sediment as Mn-containing carbonates. Iron-oxides did not undergo significant reductive dissolution. The top of the newly deposited turbidite formed an oxic layer, which was rapidly enriched in metal-oxides. The enrichment of manganese oxides was mostly due to the oxidation of dissolved Mn^{2+}, which diffused from below. The enrichment of iron oxides is explained both by the oxidation of the upward flux of dissolved Fe^{2+}, and by the input of detrital iron oxide after, or as a result of the turbidite deposition.

1. Introduction

The deposition of turbidites in marine environments results from gravity flows triggered by mass wasting events, during which several centimeters or meters of new sedimentary material can be rapidly deposited on top of autochthonous sediments (Bouma, 1962; Mulder and Cochonat, 1996). The gravity flow may either erode the previous sediment-

1. Département de Géologie et Océanographie, UMR 5805 EPOC, Université Bordeaux I, Avenue des Facultés, 33405 Talence Cedex, France. ***email: anschutz@epoc.u-bordeaux.fr***

2. Present address: Laboratory for the Study of Recent and Fossil Bio-indicators, Angers University, 2 Boulevard Lavoisier, 49045 Angers Cedex 01, France.

3. School of Ocean and Earth Science, Southampton University, Southampton Oceanography Centre, Waterfront Campus, European Way, Southampton, SO14 3ZH, United Kingdom.

water interface, or preserve it below the newly deposited sediments. In both cases the ongoing biogeochemical and biological processes will be strongly disturbed. The aim of this paper is to study these changes, especially those affecting the redox state of the dominant elements, and the biological response to the disturbance, evidenced by benthic foraminifera, a dominant element of deep-sea meiofauna (Gooday *et al.,* 1992).

One of the major biogeochemical changes accompanying turbidite emplacement is the isolation of the former sediment-water interface from oxygenated seawater. For example, Fe- and Mn-oxides are solid in oxic conditions, and are generally enriched in the oxic layer at the top of the sediment. In case of a rapid oxygen depletion of the sediment-water interface, the metal oxides may either dissolve and migrate through the sediment column (Mucci and Edenborn, 1992), or they may persist for years and form an oxic barrier for reduced species at depth within the sediment. The return to steady-state conditions at the fossilized interface will depend on the relative proportion of reduced and oxidized species and the kinetics of the biogeochemical processes. Several studies have described non-steady-state diagenesis linked to the deposition of turbidites. Most of these papers describe modifications of the sediment geochemistry caused by turbidite deposition on a millennial time scale (e.g. Wilson *et al.,* 1985; DeLange, 1986; Buckley and Cranston, 1988; Thomson *et al.,* 1998) or, at best, a decadal time-scale (Mucci and Edenborn, 1992). Observations of the evolution of redox-sensitive species toward a new steady state have only been described for a sediment layer deposited in Saguenay fjord after a catastrophic flash flood in 1996 (Deflandre *et al.,* 2000; 2002).

Benthic foraminiferal colonization has been studied intensively in nearshore and in laboratory settings. An excellent overview of the most significant results is given by Alve (1999). There appears to be an important difference between two types of environments. In areas with a high hydrodynamic energy (current velocities $>$ 20 cm/s), recolonization may be nearly instantaneous, and faunas comparable to those before the disturbance event may install in a couple of days. In low energy environments (current velocities $<$ 10 cm/s), on the contrary, it may take many months, or even years to arrive at faunas with a density, species variability and equitability comparable to the original faunas. In this case, a classical ecological succession develops, with a first colonization of a low diversity opportunistic pioneer fauna, followed by several intermediate faunas, before arriving at the highly diverse, specialized climax community (Alve, 1999). Certain negative aspects of the newly available environment, such as the presence of anoxic conditions, or strongly diminished food availability, may cause significant delays.

Few data (see Alve, 1999 for an overview) exist on foraminiferal re-colonization of deep-sea environments. Hess and Kuhnt (1996) conclude that even several years after the 1991 Mt Pinatubo ashfall, the faunas were still far from total recovery. Very little information is available about re-population after turbidite deposition. Jorissen *et al.* (1994), who studied live foraminiferal assemblages in Wilmington and South Hayes Canyon (off New Jersey, USA), conclude that the rather poor, low diversity, and surface living faunas represent a first stage of ecosystem colonization. They speculate that in these

very active canyon environments foraminiferal faunas will often remain in early colonization stages, and will not fully recover. Therefore, it is very difficult to define the characteristics of the climax community.

The top of the sedimentary sequence recovered at 650 m water depth in the canyon of Capbreton contains a turbidite, presumably deposited only a few months before sampling (Mulder *et al.,* 2001). The most probable natural event capable of triggering the turbidity current was the violent storm that affected the southern French Atlantic coast on the 27th of December 1999. The material collected on the 2nd of May 2000 gives us the opportunity to study the transient behavior of redox sensitive species in the buried sediment-water interface and the biogeochemical properties of the newly formed sediment-water interface. Furthermore, it allows us to observe the state of foraminiferal recolonization 4 months after the disturbance event, which created a more or less abiotic environment, which will subsequently be recolonized.

2. Material and methods

The studied sediment was collected with an SMBA multi-corer in the southeastern part of the Bay of Biscay, at 647 m depth (station K), in the axis of Capbreton canyon (Fig. 1), on the 2nd of May 2000, during cruise Oxybent 10. The bottom waters are North Atlantic Central Waters, with an *in situ* temperature of 10.7°C (Ogawa and Tauzin, 1973). Capbreton canyon is one of the largest European submarine valleys. The axis is a location of turbidite deposition (Nesteroff *et al.,* 1968). The SMBA multi-corer allowed us to sample the first decimeters of the sediment, the overlying bottom waters, and the undisturbed sediment-water interface, in a 10 cm diameter plexiglas tube. Overlying water samples were collected immediately after core recovery for dissolved O_2 measurements, using the Winkler titration method (Strickland and Parson, 1972). Profiles of pore water O_2 were measured on board using a cathode-type mini-electrode (Revsbech and Jørgensen, 1986; Helder and Baker, 1985; Revsbech, 1983). The measurement was performed at a 1 mm step 5 mm above the sediment-water interface, within the bottom water recovered with the multi-tube device, and 20 mm below, in the sediment. It was completed within 15 min after core recovery. Subsequently, the core used for O_2 profiling was sliced in thin horizontal sections (0.5 cm for the top 2 cm, 1 cm below, and 2 cm at the bottom) within 90 minutes. For each level a sub-sample was immediately sealed in a pre-weighed vial and frozen under inert atmosphere (N_2) for further analyses of porosity and solid fraction. Another subsample was centrifuged under N_2 at 5000 rpm during 20 min in order to collect pore waters. Two aliquots of water were filtered (0.2 μm) and frozen at −25°C for nutrient analyses, and the other aliquot was filtered and acidified with ultrapure HNO_3 for dissolved Mn and Fe analyses. This sub-sampling has been used routinely for all cores of the eleven Oxybent cruises (Anschutz *et al.,* 1999). The vertical resolution for pore water analyses is high at the top and slightly poorer below. However, our sampling procedure allowed us to extract three samples below the recent turbidite. A second tube of the same multi-core employment was brought back to the laboratory and opened (in late May 2000) for

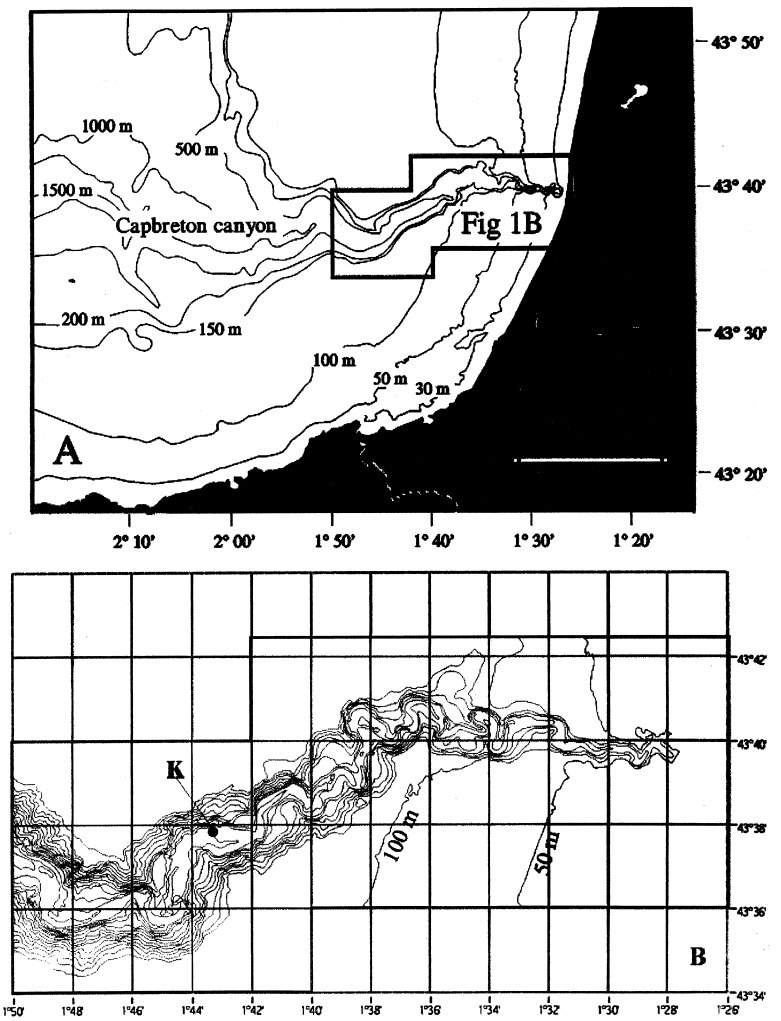

Figure 1. A. Map of the Southeastern part of the Bay of Biscay showing the Capbreton canyon. B. Detailed map of the study area showing the location of the Station K. Isobaths at 50 m intervals (from Mulder *et al.,* 2001).

sedimentological observations and high-resolution sub-sampling of the solid fraction. A third core was sampled for benthic foraminifera immediately upon retrieval. The top ten centimeters of the core were sliced, the 0–1 cm interval into 0.25 thick slices, the 2–4 cm interval into 0.5 cm slices, and the 4–10 cm interval into 1 cm thick slices. Sediment was stored in 250 ml bottles, which were filled with 95% ethanol and contained 1 g/l Rose-Bengal stain (Lutze and Altenbach, 1991). In late May 2000, the five cm below the turbidite were sampled in the second tube (see before), and underwent the same treatment.

Foraminiferal samples were sieved through 63 and 150 μm mesh screens. All sieve fractions were preserved in 95% ethanol. Foraminifera were picked from a solution of 50% ethanol, and stored in Chapman slides. When we discovered the presence of a recent turbidite, about three weeks after sampling, new samples were collected immediately below the turbidite. This paper concentrates on the foraminifera found in the >150 μ fraction. The concentration of living (stained) benthic foraminifera as well as planktonic foraminifera is expressed as the number of individuals per 50 cm^3.

The activities of ^{210}Pb and ^{234}Th were determined in freeze-dried samples by gamma counting. The excess activity of ^{210}Pb was calculated from ^{226}Ra-supported ^{210}Pb deduced from the activities of ^{214}Pb and ^{214}Bi. Porosity was determined by comparison of the weights of wet and freeze-dried sediment. The freeze-dried solid fraction was homogenized and the water content used to correct the analyses for the presence of sea salt.

Particulate sulfur (S_{tot}) and total carbon were measured on the dry sediment using a Leco C/S 125. Inorganic carbon (C_{inorg}) was measured by automated calcimetry with 6N HCl from 250 mg of powdered sample. Organic carbon (C_{org}) is calculated as the difference between total carbon and C_{inorg}. Wet samples were subjected to an extraction technique for the determination of reactive particulate Fe- and Mn-oxides. The most reducible fraction was extracted with an ascorbate solution buffered at pH 8 (Ferdelman, 1988; Kostka and Luther, 1994; Anschutz *et al.,* 1998). About 1 g of wet sample was leached with a 25 ml solution during 24 hours while shaking continuously at room temperature. Iron extracted with ascorbate (Fe_{ASC}) comes from amorphous iron oxides. Specific tests on particulate-Mn extraction with ascorbate (Mn_{ASC}) have not yet been published. It has been shown in our laboratory, however, that it represents the complete fraction of Mn-oxides. Mn_{ASC} is extracted at pH 8, which suggests that Mn-carbonates are not leached. Mn and Fe were measured by flame atomic absorption spectrometry.

Interstitial water compounds were analyzed using techniques adapted for small volumes of samples. Nitrate was measured by flow injection analysis (FIA) according to Anderson (1979). Ammonia was analyzed with the FIA method described by Hall and Aller (1992). Dissolved Fe was measured with the colorimetric method using ferrozine (Stookey, 1970). Dissolved Mn^{2+} was determined by atomic absorption spectrometry. The pH was measured onboard with an electrode calibrated using three NBS buffers and a synthetic seawater TRIS buffer solution.

3. Results

a. Core description

Macroscopic observation of the core shows three sedimentary units noted S1, S2 and S3 from top to bottom. A detailed description of these sedimentary sequences, based on an X-ray imaging system and grain size measurements, was presented earlier by Mulder *et al.* (2001). The two topmost units, S1 and S2, are separated by an erosive contact; also the contact between units S2 and S3 is rather sharp. Ocher (10YR 6/5) oxidized layers

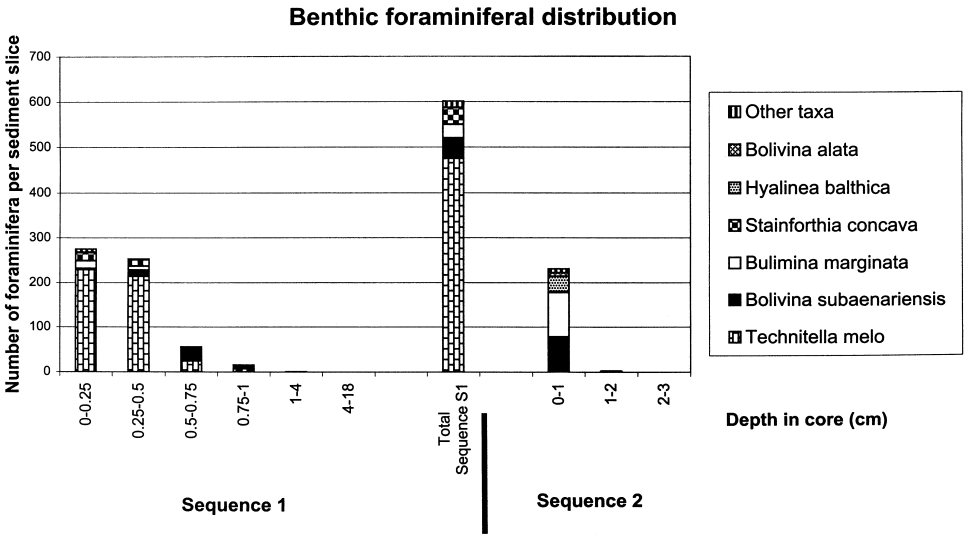

Figure 2. Vertical distribution of Rose-Bengal stained benthic foraminiferal tests. Numbers are given per 50 cm^3.

containing Rose-Bengal stained benthic foraminifera are located below the contact between S1 and S2. Sequence S3 is a fining-up sequence with its base missing due to insufficient coring depth. Grain size grades up from fine sands to clayey silts. Sequence S2 is 5 cm thick. It contains only a fine silty clay facies with slight bioturbation at its top, overlain by an oxidized layer. Sequence S1 is the most complete one. It is 18-cm-thick, fining-upward, and shows a clean sandy facies with mud clasts at the base, above an erosive basal contact. This 3 cm thick basal part is overlain by a facies with convolute laminations and by a facies with parallel laminations. The latter facies is marked by an increase of porosity. The sequence ends with a 6 cm thick silty-clay facies similar to the facies observed in S2 with slight bioturbation in the top centimeter. A 1 cm-thick oxidized facies has developed at the top of the core. The facies succession and the progressive fining-up trend suggest that the three sequences observed in core K correspond to classical Bouma sequences (Bouma, 1962; Shanmugam, 1997). The unlaminated facies at the top of the three sequences is interpreted as the composite of the finest, topmost part of the turbiditic facies and the hemipelagic, clay sedimentation in the months following turbidite deposition.

b. Foraminiferal distribution

Sequence S1 contains a fairly rich stained benthic foraminiferal fauna, which is entirely concentrated in the oxic layer (Fig. 2, Table 1). The bulk of the live specimens (88%, 528 out of 601) are even found in the first two 0.25 cm levels. The fauna is strongly dominated by *Technitella melo,* which accounts for 79% of the total. *Stainforthia concava* (6%),

Table 1. Number of Rose-Bengal stained benthic foraminifera per sediment slices and the abundance of planktonic foraminifera.

Station OB10-K	*Technitella melo*	*Bolivina subaenariensis*	*Bulimina marginata*	*Stainforthia concava*	*Hyalinea balthica*	*Bolivina alata*	Other taxa	Total benthic foraminifera	Planktonic foraminifera	Planktonic forams/10cc
0–0.25	229	3	17	18	1		7	268	51	32,38
0.25–0.5	214	14	9	14			2	251	59	37,46
0.5–0.75	24	23	3	3			3	53	46	29,21
0.75–1	7	5	1	1			2	14	47	29,84
1–4	1						0	1	32	10,16
4–18							0	0	8	1,27
0–1		78	100	1	35	8	9	222	101	16,03
1–2		1	1				1	2	77	12,22
2–3							0	0	12	1,90
Total Sequence S1	475	124	131	37	36	8	24	811	433	
Total Sequence S2	0	79	101	1	35	8	10	224	190	

Bulimina marginata (5%) and *Bolivina subaenariensis* (7.5%) are the main accompanying taxa. The former two species are mainly present in the first two 0.25 cm levels, whereas *B. subaenariensis* is found slightly deeper, and has a maximum in the 0.5–0.75 cm level. Eight rarer taxa account for the remaining part of the fauna. Planktonic foraminiferal tests (Fig. 3) are fairly abundant in the first cm (about 150 tests per 50 cc), in the second cm their density drops to about 50 tests per 50 cc, and in all deeper levels only trace quantities are found.

The top of sequence S2 was sampled in less detail. The topmost 0–1 cm level contains 231 weakly stained specimens, the 1–2 cm only 3 weakly stained specimens. The fauna is dominated by *B. marginata* (43%), *B. subaenariensis* (34%) and *Hyalinea balthica* (15%). Six other rare taxa complete the assemblage. Planktonic foraminiferal tests are relatively abundant (50–70 tests per 50 cc) in the first 2 cm; only trace quantities were found in deeper layers (Fig. 3).

c. Geochemistry

With its very short half-life of 24 days, $^{234}Th_{exc}$ should be present only at the water-sediment interface. The top of S1 has an extremely high $^{234}Th_{exc}$ activity, of 3600 Bq/kg. However, the activity remains high in the top 6 cm of the core (Fig. 4), suggesting an efficient mixing of the sediment. The preservation of the turbiditic sequences (Mulder *et al.,* 2001) suggests that the post-depositional mixing of the particles was low.

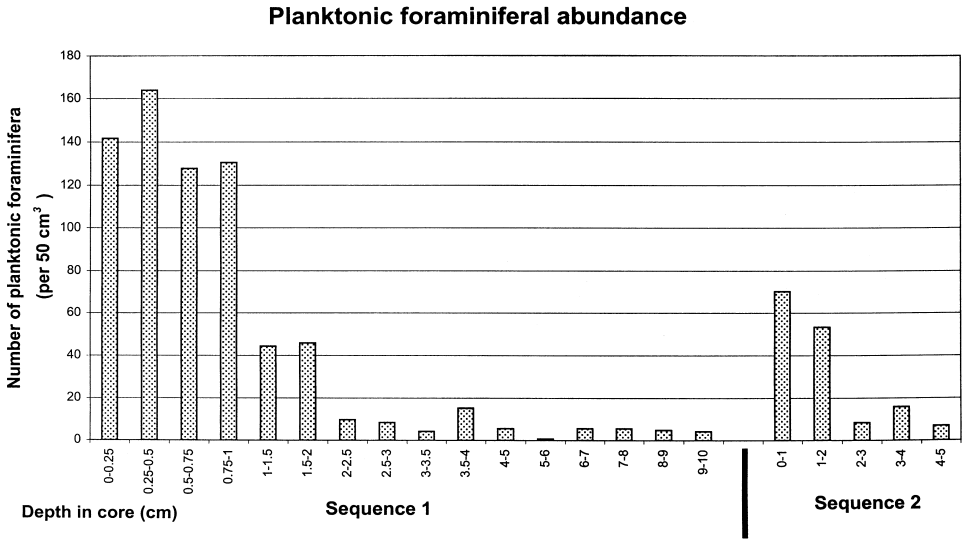

Figure 3. Vertical distribution of planktonic foraminiferal tests, standardized for a sediment volume of 50 cm^3.

The activity of $^{234}Th_{exc}$ detected below the sediment-water interface is probably a residue of the ^{234}Th, which has been trapped on the fine particles during the turbiditic event, and before their settling. The detectable activity of $^{234}Th_{exc}$ indicates that the turbidite has been deposited within less than a few months before core collection. Also the interface between S1 and S2 shows a high $^{234}Th_{exc}$ activity. This suggests that this former sediment-water

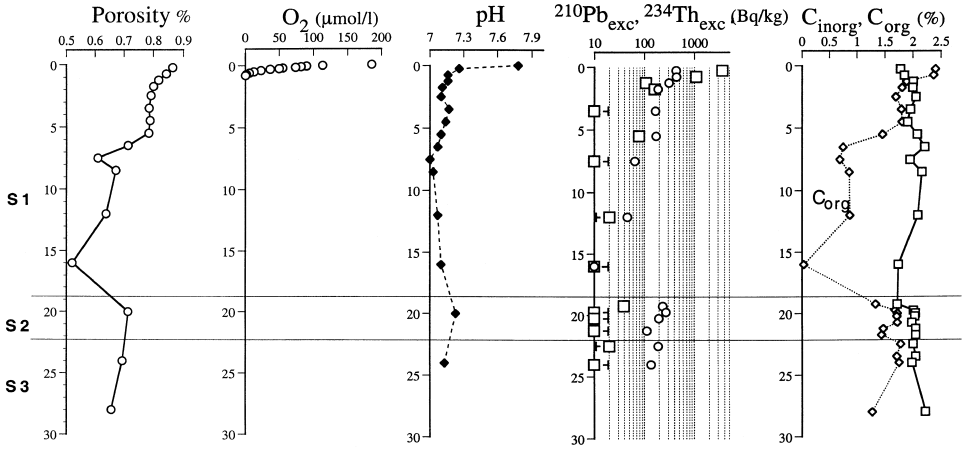

Figure 4. Vertical profiles of porosity in %, pore water O_2 in µmol/l, pH, organic carbon (C_{org}), and inorganic carbon (C_{inorg}) in weight percent of dry sediment corrected for salt content, and excess ^{210}Pb (circles) and ^{234}Th (squares) in Bq/kg in the sediment of the Station K.

interface has been covered very recently by the turbiditic sequence S1. The most probable natural event able to trigger the turbidity current is the violent storm that affected the southern Atlantic coast of France the 27th of December 1999 (Mulder *et al.,* 2001). Therefore, the time elapsed between the turbidite event and the core sampling was probably 127 days. 127 days corresponds to more than 5 half-lives of the radioactive decrease of ^{234}Th, which indicates that the activity of $^{234}Th_{exc}$ at the top of S2 was close to 1600 Bq/kg at the time of the turbidite emplacement. Such a high activity is common for the top sediments of the Capbreton canyon (Hyacinthe *et al.,* 2001). The top parts of S1 and S2 show a high $^{210}Pb_{exc}$ activity (half-life of 22.3 years) (Fig. 4). The $^{210}Pb_{exc}$ activity decreases at the bottom of S1. In a sedimentary sequence, where the grain size grades up, the $^{210}Pb_{exc}$ activity cannot be directly related to the accumulation rate and the continuous radioactive decay. The activity also depends on the $^{210}Pb_{exc}$ inventory at the moment of the sediment deposition. The grain size is a parameter, amongst others, which determines the amount of $^{210}Pb_{exc}$ adsorbed on particles. In the sequence S1, the downward decrease of the $^{210}Pb_{exc}$ activity can be related to the increase of grain size.

The dissolved O_2 concentration in the bottom water was 202 μmol/l, which corresponds to concentrations measured earlier at this water depth (Ogawa and Tauzin, 1973). Oxygen concentration decreased 2 mm above the sediment-water interface and reached the zero level at only 7 mm depth, and remained at zero deeper down. The bottom water pH was 7.78. It dropped to 7.26 in the upper part of the core and continued to decrease below to values between 7.2 and 7.0. The pH increased again to 7.23 in the sample located just below the S1–S2 interface (Fig. 4).

The organic carbon content is above 1.5 wt% at the top of S1 and S2 (Fig. 4). The concentration drops below 1 wt% in the silty and sandy facies in the lower part of S1. It was close to 0 at 16 cm depth at the bottom of unit S1. The C_{inorg} concentration of the sediment has a mean concentration of 2.0 wt%. This concentration does not vary significantly along the profile. However, values lower than 1.8% were measured at the very top of the core, at the top of the S1–S2 interface, and at the sandy bottom of S1.

The nitrate concentration was close to 15 μmol/l in the bottom water and decreased sharply within the oxic layer to values lower than 2 μmol/l (Fig. 5). We observed a peak of 5 μmol/l at the bottom of S1. The concentrations of dissolved NH_4^+ were below the detection limit in the bottom water and they increased in a regular manner in the upper part of the S1 unit. They reached a concentration above 600 μmol/l below unit S1 (Fig. 5).

Dissolved manganese became detectable in samples where the oxygen concentration reached values close to zero. Below, the Mn^{2+} concentrations increased sharply to values which stay close to 50 μmol/l. The sample located at the top of S2 had a concentration peak of 110 μmol/l (Fig. 5). The profile of dissolved Fe was more irregular than that of Mn^{2+}. Dissolved iron appears 5 mm below dissolved manganese. It increases below to concentrations up to 650 μmol/l. Dissolved iron decreases at the bottom of unit S1 but increases again to 200 μmol/l in unit S2.

The profiles of reactive metal oxides extracted with ascorbate (Fig. 5) shows maximal

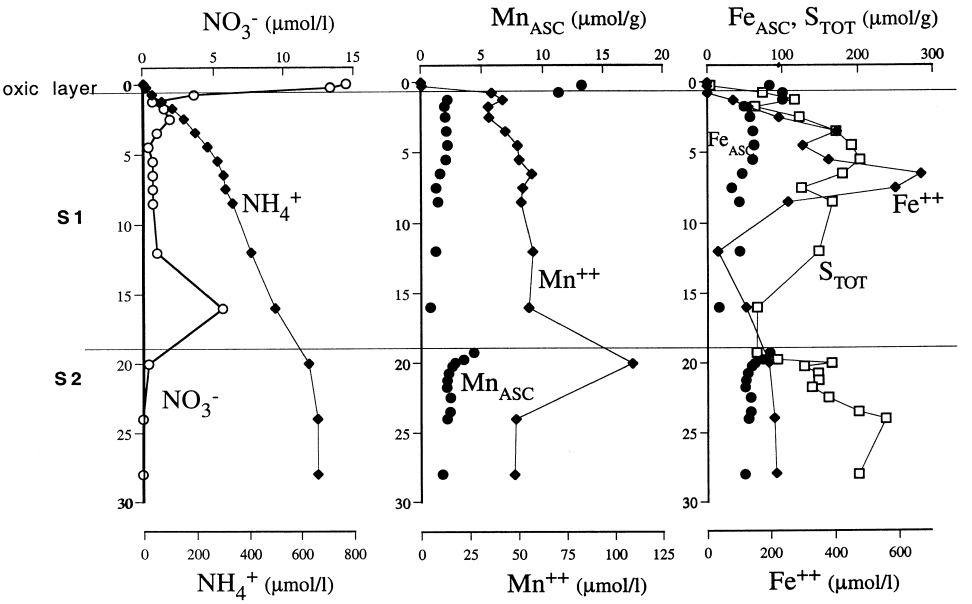

Figure 5. Vertical profiles of redox sensitive species in sediments of the Station K. The pore water compounds are given in µmol/l (NO_3^-, NH_4^+, Mn^{2+}, Fe^{2+}). The value indicated at depth 0 cm represents the value measured in the bottom water. The reactive particulate phases are given in micromole per gram of dry sediment (µmol/g) and correspond to ascorbate extractable manganese (Mn_{ASC}) and iron (Fe_{ASC}), and total sulfur (S_{tot}).

values in the top centimeter of the core for Mn and in the top 1.5 cm for Fe. The concentrations decrease abruptly to intermediate values in the unlaminated and high porosity facies between 1.5 and 6 cm. The lowest concentrations are measured in the silty and sandy facies in the bottom part of S1. A second maximum of Fe_{ASC} and Mn_{ASC} is detected in the top cm of the unit S2.

Solid sulfur represents less than 20 µmol/g in the oxic part of the core. The concentrations increase below the oxic layer. The shape of the S_{TOT} profile in the S1 unit is very similar in shape to the Fe_{ASC} profile.

4. Discussion

a. Rose Bengal staining

Rose Bengal stain is commonly used for the recognition of live benthic foraminifera. This non-vital stain, which attached to proteins, ideally provokes a bright pink color. Unfortunately, rose Bengal will stain both healthy and necrotic protoplasm, as well as bacterial films at the test interior (Bernhard, 1988; 2000). Because of interspecific differences in staining intensity, criteria have to be selected for each taxon. But even within a taxon, important variability of staining intensity may be found, increasing the subjectivity

of the method. Nevertheless, the rose Bengal technique is still the only methods, which allows us to recognize the living foraminifera in large assemblages of mixed (alive and dead) foraminiferal tests.

Because of the appearance of fairly rich stained faunas in anoxic sediments, several authors (e.g. Douglas *et al.,* 1978; Corliss and Emerson, 1990; Jorissen *et al.,* 1995) have questioned whether these stained tests really correspond to live individuals, or, rather, to dead specimens which were preserved in anoxic conditions, where protoplasm decay may be a relatively slow process. Douglas *et al.* (1980) estimated that about 30% of stained foraminifera found in anoxic sediments in Santa Monica Basin, showed signs of protoplasm decay, and were probably dead at the time of collection. Bernhard (1988) showed that foraminifera still stained four weeks after their death in oxic conditions. Corliss and Emerson (1990) estimate maximum values for the protoplasm decay period of 0.07–2 years at the oxic sediment-water interface, and 2–80 years in deeper sediment layers. Unfortunately, none of these authors mention how exactly the protoplasm of dead foraminifera is stained. In our experience (which is based on the analysis of the faunas of more than 50 stations down to 5 to 10 cm depth in the sediment), most specimens found at the sediment surface, have all chambers clearly stained (often with the exception of the last chamber). But also for these presumable living specimens, the brightness of the staining is very variable between species. In specimens sampled in well oxygenated sediments, the difference between stained and unstained specimens is obvious, protoplasm degradation is apparently rapid, and the subjectivity involved in the quantification of the living fauna is minimal. In the deeper, dysoxic or anoxic sediment layers, a wide range of staining intensities can be found. Some specimens are still brightly stained, in others, perhaps recently dead specimens with necrotic protoplasm, staining is duller, and in still other specimens, perhaps with a more advanced state of protoplasm decay, only a few chambers are weakly stained. It is evident that the quantification of the live faunas is more subjective here. The risk of identifying important amounts of dead foraminifera as living one can be minimized by the application of very strict staining criteria, based on observations on the staining of the same species in the surface sediment layer.

Unfortunately, the faunas from sequence S2 were only stained about 4 weeks after core retrieval. Therefore, the weakly stained specimens found in the top of this sequence, all of which are rejected as living by our usual staining criteria, cannot be interpreted unambiguously. The faunas may have still been alive at the time of sampling, and in that case the weak aspect of the staining could be due to partial protoplasma degradation in the four weeks following sampling. A second, in our opinion more probable, possibility is that dead specimens still stained weakly several months after the deposition of the turbidite, and the ensuing death of the foraminifera. This prolonged period of time can be explained by the fact that the sediment at the top of sequence S2 rapidly became anoxic after the deposition of sequence S1. In both cases, the presence of these weakly stained foraminifera confirms that the deposition of sequence S1 took place in the recent past. Unfortunately, this

information does not allow us to precise the period elapsed since the death of the foraminiferal fauna.

b. Benthic foraminiferal recolonization

The recent fauna is strongly dominated by *Technitella melo.* This rather poorly known agglutinated taxon has been described from low oxygen environments (Bernhard, 1992). In the Bay of Biscay, the taxon has never been encountered in any of the other ten sampling stations (e.g. Fontanier *et al.,* 2002). The accompanying three taxa are more common, and are typical of the Capbreton canyon area. *Bolivina subaenariensis, H. balthica* and, to a lesser degree, *Bulimina marginata* strongly dominate the extremely rich live faunas (up to 8600 specimens under a 72 cm^2 surface) sampled at station G, positioned in the Capbreton Canyon at 450 m depth (unpublished data). *B. subaenariensis* has been described as a major species in an assemblage influenced by periodic upwelling off Florida (Sen Gupta *et al.,* 1981). *S. fusiformis* is considered as an opportunistic early colonizer (Alve, 1994; 1999). Many other references show the success of these taxa in high productivity (and sometimes low oxygen) environments, confirming the opportunistic behavior of these taxa.

We think that both the surface fauna and the fauna at the top of turbiditic sequence S2 correspond to an early stage of ecosystem colonization. The very low species diversity, the sediment surface microhabitats and the opportunistic behavior of the dominant taxa strengthen our opinion. These early stages of colonization would mean that the periods of time between the successive turbiditic sequences is in most cases too short to reach more mature faunas. A similar phenomenon was observed in Wilmington Canyon (Western Atlantic), where low foraminiferal densities and a total absence of foraminifera below the first cm were explained by the physical instability of the canyon environment, keeping the faunas in an early stage of colonization (Jorissen *et al.,* 1994).

In the case of Capbreton canyon station K, *Technitella melo,* which we never observed in our other ten stations from the Bay of Biscay, was probably one the first species colonizing the abiotic environment after the deposition of the turbiditic sequence S1. In more advanced stages of ecosystem colonization, represented by the slightly more diverse fauna on top of sequence S2, this taxon is probably absent because of its lower competitive abilities in comparison with other taxa. We speculate that *T. melo,* which is otherwise a very rare species, strongly dominates the recolonizing assemblage, because it may be adapted to the rather specific conditions following turbidite deposition. The turbiditic sediment is composed of silts with about 1.8% of organic matter. Although this concentration of organic matter is very high for deep sea sediments, visual inspection suggests that it concerns mainly plant debris. Since cellulose is not metabolisable without the intervention of fermenting anaerobic microbial communities (Fenchel and Finlay, 1995), it is possible that despite the elevated percentage of organic matter, the environment was very oligotrophic in the first days after turbidite deposition. We speculate that *T. melo* could be a species specialized in colonizing such an oligotrophic environment. The eventual absence of

suitable food particles in an initial colonization stage of colonization could also explain the relatively long recovery time.

The absence of *T. melo* in the living as well as dead assemblages of sequence 2 is intriguing. It seems highly improbable that the species was living here in December 1999, just before turbidite deposition, and that all tests subsequently disintegrated (a common phenomenon for certain agglutinated taxa) in the few months following turbidite deposition. Another possibility would be that the completely population of this surface-living taxon was swept away during turbidite deposition, together with the topmost millimeters of the sediment. However, also this possibility is very unlikely in view of the presence of living *T. melo* down to 1 centimeter, and the absence of a clear vertical species succession in the recent fauna. Therefore, we conclude that for an unknown reason, *Technitella melo* did not make part of the foraminiferal fauna recolonizing turbiditic sequence S2.

c. Depth of bioturbation

The planktonic foraminiferal record shows a clear two-stepped density-profile. The maximum densities (about 150 specimens/50 cc) in the topmost 0.5 cm of sequence S1, are interpreted as the result of a direct input by hemi-pelagic sedimentation after the deposition of turbiditic sequence S1. The intermediate densities (about 50 specimens/50 cc) found between 0.5 and 1 cm, on the contrary, are probably the result of downward mixing by the benthic fauna. This is confirmed by the presence of scarce live benthic foraminifera in this depth interval. The same interpretation is probably valid for sequence S2. The relatively low density, of planktonic as well as benthic foraminifera, in the topmost cm suggests the top of sequence S2 comprises only the lower part of the former hemipelagic sediment. The upper part (a few mm) of sequence S2 has probably been eroded during the deposition of turbiditic sequence S1. The slightly lower numbers (about 50 specimens/50 cc) in the 1–2 cm level of sequence S2, suggests that these tests have been introduced there by bioturbation. Below the second cm of sequence S2, only trace quantities of planktonic foraminifera are found.

d. The distribution of redox species

i. The establishment of the anoxic condition. The arrival of a turbidity current provokes a mixing of allochthonous particles, pore waters, and oxic bottom waters. The composition of the interstitial waters and sedimentary particles of core K is the result of the geochemical reactions and diffusive transport of dissolved compounds since the deposition of the turbidite. The disappearance of oxygen in almost the entire core, and particularly at the previous interface at the top of unit S2, indicates that enough time has elapsed to allow the consumption of all free oxygen by oxidation of reduced species, like Fe-sulfide, or organic carbon through oxic respiration. The high organic carbon concentrations (around 2%) suggest that the O_2 consumption was probably fast. We have conducted an experiment in which anoxic sediments, collected from a neighboring station with a very similar concentration of organic carbon, were vigorously mixed with O_2-saturated seawater with a

fresh sediment:seawater volume ratio of 1:1. After 24 hours, O_2 was totally consumed. This experiment confirms that O_2 will be rapidly consumed after isolation of the sediments from oxygenated bottom waters, and explains the absence of free oxygen below the several month old turbidite.

The presence of reduced dissolved species in unit S1 could result from diffusion of these species from below. However, dissolved Fe does not show a diffusion profile. It shows a layer where dissolved Fe is produced, probably due to the reduction of particulate Fe(III) phases, located in the first decimeter below the oxic layer. Therefore, anaerobic processes occur in the newly deposited unit S1, where oxic particles are reduced. We have observed concentrations of Fe_{ASC} above 50 μmol/g in unit S1, which indicates that reactive Fe(III) phases are available to sustain the reaction of Fe(III) reduction. The particulate sulfur profile follows the Fe_{ASC} profile. Therefore, reactive Fe(III) phases may have resulted from the partial oxidation of iron sulfide after the mixing of reduced and oxic sediments during the turbidite event. Both dissolved oxygen or particulate Mn-oxides are potential oxidants for iron sulfides.

ii. The new oxic layer. The high concentrations of Mn_{ASC} and Fe_{ASC} at the top of the core results first from an accumulation of Mn- and Fe-oxides linked to the oxidation of dissolved Mn(II) and Fe(II) diffusing upwards from the anoxic sediment, and second, from the deposition of oxides with detrital particles of background sedimentation after turbidite deposition. The first process occurs, since we have observed a concentration gradient of dissolved Fe and Mn. The establishment of such an oxic layer by the diffusion process needs time. The time required for this accumulation of oxides can be estimated using a diffusion model, assuming that the detrital input was zero, and the gradient of dissolved Fe and Mn remained constant during time. This assumption is probably erroneous, but it allows us to calculate a rough maximum age for the turbidite.

First we have calculated from the porosity and concentration data the excess of Mn_{ASC} and Fe_{ASC} present in the oxic layer of the sediment in comparison with the underlying sediment. In a surface section of 1 cm^2, the excess of Mn is 4.4 μmol and the excess of Fe is 20 μmol. The comparison of these values with a diffusive flux expressed in μmol per cm^2 per unit time allows us the estimation of the time required to develop the observed metal-oxide enrichment.

The fluxes of species dissolved in pore waters can be calculated, assuming transport by molecular diffusion, from the concentration gradients according to Fick's first law: $J = -\phi D_s dC/dX$, where J is the flux, ϕ is the porosity, dC/dX is the concentration gradient, and D_s is the bulk sediment diffusion coefficient corrected for tortuosity, i.e. $D_s = D_o/\theta^2$ where θ is the tortuosity and D_o is the diffusion coefficient in water (Berner, 1980). D_o values were obtained from Li and Gregory (1974) and the value of θ^2 is assumed to equal to $1 - \ln(\phi^2)$ (Boudreau, 1996).

The concentration gradient of dissolved Mn occurs at about 1 cm depth. At this depth the calculated D_s of Mn is 3.48 10^{-6} cm^2/s. The concentration gradient is difficult to estimate

accurately, because it occurs within two successive 0.5 cm-thick samples. The concentration of dissolved Mn is 36 μmol/l in the 1–1.5 cm sediment slice and close to zero μmol/l in the 0.5–1 cm slice. Therefore the decrease of 36 μmol/l occurs within 0.5 cm at the most, and probably less. Then, the calculated gradient is at least 72 nmol/cm^4. The diffusive flux calculated with this minimum value is 0.213 pmol/cm^2/s. This flux can supply the Mn in excess in the oxic layer within 8 months. If we consider a concentration gradient, which is twice higher than the estimated minimum value, then, the excess Mn is supplied in 4 months, which corresponds approximately to the time elapsed between the core sampling and the estimated date of turbidite formation in December 1999. Therefore, this constant diffusion model accurately explains the peak of particulate Mn in the oxic layer.

The concentration gradient of dissolved Fe is linear between 3.5 and 1 cm depth. The diffusion flux calculated from this gradient is 0.443 pmol/cm^2/s. This flux supplies the excess of Fe present in the oxic layer in 1.4 years. This value is higher than the time estimated for Mn. This suggests that the processes that control the enrichment of metal oxide at the top of newly deposited sediments are not quantitatively the same for Mn and Fe. An important part of the Fe in excess probably originates from a downward flux of sedimenting Fe(III) particles rather than exclusively from an upward flux of dissolved Fe. It is also possible that the profile of dissolved Fe is not at steady state.

iii. The previous sediment-water interface. The top of S2 unit is also enriched in Mn_{ASC} and Fe_{ASC}. This suggests that the sediment-water interface formed prior to the deposition of unit S1 has only been eroded very weakly, or even not at all. However, both sedimentological (erosive contact) and foraminiferal evidence argue for erosion of the top millimeters. The presence of metal oxides indicates that they have not been totally reduced within the few months after being buried in an anoxic environment. The profile of dissolved Mn shows however a maximum concentration in the sample located at the top of S2. This peak clearly indicates that Mn-oxides were being reduced at the time of core sampling. Except this peak, the background concentration of dissolved Mn in the core is relatively constant, and close to 50 μmol/l. Therefore, the concentration of Mn is probably controlled by an equilibrium with a solid phase. The removal of dissolved Mn could be related to the precipitation of secondary Mn-containing carbonates. The precipitation of authigenic carbonates is favored by the production of alkalinity linked to anaerobic mineralization of organic carbon (Mucci *et al.,* 1999). Dissolved manganese is most likely precipitated as a mixed calcium-manganese carbonate (Middelburg *et al.,* 1987) as the pore waters become supersaturated with respect to both calcite and rhodochrosite following the production of carbonate alkalinity via sulfate reduction. At the top of S2, the higher concentration of dissolved Mn, but also the higher pH, indicates that interstitial waters are supersaturated here with the Mn-bearing-carbonate phase. The peak of dissolved Mn is limited to the sample located near the top of S2. One can expect that shoulders of this peak should be present above and below this level due to the diffusive transport of the

concentration anomaly. In a purely diffusive transport, the vertical distance z of the concentration anomaly growing ahead of the reductive dissolution zone depends on time t and the coefficient of diffusion D_s according to the Einstein relation (Boudreau, 1997), where $z = (2D_s t)^{0.5}$. Considering an age of the turbidite S1 of four months, the concentration anomaly should be detectable about 7 cm above and below the top of S2. The peak of dissolved Mn is much thinner. Therefore, Mn^{2+} is probably trapped as an authigenic phase close to the S1–S2 interface. This suggests that the current reductive dissolution of Mn-oxide at the paleo-interface produces an environment, which is temporarily supersaturated with a Mn-carbonate phase, probably due to kinetic effect of carbonates precipitation, but the Mn-carbonate becomes the definitive sink of Mn.

The profile of dissolved iron shows no peak at the top of S2. This suggests that, unlike Mn, Fe-oxides are not, or only very weakly, reduced at the paleo-interface. They appear to be more refractory and are not transformed to another authigenic phase within four months. Manganese oxides and oxyhydroxides are oxidants for Fe^{2+} (Myers and Nealson, 1988; Postma, 1985; Hyacinthe *et al.,* 2001), which can explain the removal of Fe^{2+} and a part of the reductive dissolution of particulate Mn.

iv. Nitrate and ammonia. The new oxic interface at the top of the sediment core presents a distribution of dissolved nitrogen species, which is common in hemipelagic sediments. We observe that nitrate is present in the oxygen-containing layer and then decreases downwards, whereas ammonia concentration is close to zero at the top of the core and increases downwards in the anoxic sediment. The presence of nitrate in the oxic layer is attributed to the succession of reactions that lead to the bacterial nitrification of organic N or ammonia that diffuses from below. The consumption of nitrate below the oxic layer is due to the bacterial denitrification. The presence of a peak of nitrate at 2.5 cm depth, below the oxic layer suggests that nitrate is produced anaerobically, probably from the oxidation of ammonia with manganese oxides as suggested in several recent studies (e.g. Hulth *et al.,* 1999; Anschutz *et al.,* 2000).

The ammonia profile shows a smooth gradient from the bottom to the oxic layer. The classical explanation for this is that ammonia is produced from the anaerobic mineralization of organic N at depth. In the oxic layer, nitrifying bacteria oxidize ammonia with oxygen to nitrite and nitrate, and nitrate is subsequently reduced anaerobically to dinitrogen by denitrifying bacteria.

The top of unit S2, which corresponds to the paleo-oxic interface, presented probably similar profiles of dissolved nitrogen species prior to the deposition of unit S1, with high nitrate and low ammonia concentration. After four months, ammonia and nitrate profiles are smooth. They show no indication of the previous oxic condition. This indicates that nitrate has been rapidly consumed by denitrification, probably shortly after the consumption of all free oxygen. In the absence of O_2, ammonia produced by organic-N mineralization was allowed to accumulate in the interstitial waters. Recent publications show that ammonia may also be directly oxidized by manganese oxide, either to dinitrogen (Luther *et*

al., 1997; Hyacinthe *et al.,* 2001), or to nitrate in anaerobic sediments (Aller *et al.,* 1998; Hulth *et al.,* 1999; Anschutz *et al.,* 2000). Our profiles do not show these reactions, which should be marked by a minimum in the ammonia profile and a peak in the nitrate profile. However, the reduction of manganese oxide by ammonia cannot be excluded, first because it is thermodynamically feasible, second, because it has been observed in experiments (Hulth *et al.,* 1999) and in the field (Deflandre *et al.,* 2002). In the present case the effects of this reaction are not shown in the profile of nitrogen species, because the high concentration of labile organic matter buried at this depth probably promotes competitive reactions such as rapid denitrification and efficient organic-N mineralization to ammonia. A peak of dissolved nitrate is observed above unit S2, in the sandy and organic-C depleted part of the unit S1. This layer also contains dissolved reduced species, which probably exclude the infiltration of oxic water to this depth to explain the presence of nitrate. Here, nitrate can be anaerobically produced from ammonia oxidation with Mn-oxides. The low concentration of organic-C at this depth prevents the following utilization of the nitrate for denitrification. This hypothesis may explain the peak of nitrate, but cannot be confirmed nor ruled out. Pore water sampling with a higher vertical resolution is needed to better constrain the interactions between nitrogen and the metals after the sudden burial of an oxic sediment-water interface.

5. Conclusions

We have studied a sediment core collected in the axis of Capbreton canyon at 640 m depth. The sediment consists of a succession of three turbidite layers. Most available data suggest that the 18-cm-thick turbidite layer identified at the top was deposited only four months before core collection. The composition of the benthic foraminiferal fauna suggests that the benthic environment is still in a very early state of colonization four months after the turbidite deposition. *Technitella melo,* which has not been previously observed in the faunas of Capreton canyon, appears to be the first colonizing species. We speculate that this taxon is adapted to food-impoverished conditions dominating the benthic ecosystem in the days after turbidite deposition. The slightly more diverse fauna found in the top of unit 2 is more comparable to faunas found in other stations from the Capbreton canyon. We think that, as a consequence of repeated turbidite deposition, and the prolonged period of time needed for full ecosystem recovery, the canyon environments remain systematically in early stages of recolonization. Apparently the periods of time between the successive turbidites are too short to allow complete ecosystem recovery.

The top of the newly deposited turbidite forms an oxic layer, which is rapidly enriched in Mn- and Fe-oxides. The enrichment of manganese oxides is mostly due to the oxidation of dissolved Mn^{2+}, which diffuses from below. The enrichment of iron oxides is partly explained by the oxidation of the upward flux of dissolved Fe^{2+}, but the input of detrital iron oxide after the turbidite deposition appears to be important as well.

The distribution of redox-sensitive species clearly shows that anaerobic processes of organic matter mineralization rapidly occur in the turbidite layer and in the previous oxic

sediment-water interface. Manganese oxides, which are buried under the new turbidite layer, are rapidly reduced. However, manganese remains trapped in the sediment as Mn-containing carbonates. Iron-oxides do not undergo significant reductive dissolution in the time frame observed. The behavior of nitrogen species needs further investigation.

Acknowledgments. This research is a contribution of the CNRS UMR 5805 "Environnements et Paléoenvironnements Océaniques", and was funded by the program PROOF of the Institut National des Sciences de l'Univers and the Région Aquitaine. Karine Dedieu contributed to the laboratory analyses. We are grateful to Olivier Weber, Thierry Mulder, Silvia Hess, and Pierre Cirac for several discussions that clarified the ideas developed in this paper. We thank the crew of the "Côtes de la Manche" and all the participants of the Oxybent missions.

REFERENCES

Aller, R. C., P. O. J. Hall, P. D. Rude and J. Y. Aller. 1998. Biogeochemical heterogeneity and suboxic diagenesis in hemipelagic sediments of the Panama Basin. Deep-Sea Res. I, *45,* 133–165.

Alve, E. 1994. Opportunistic features of the foraminifer *Stainforthia fusiformis* (Williamson): evidence from Frierfjord (Norway). J. Micropal., *13,* 24.

—— 1999. Colonization of new habitats by benthic foraminifera: a review. Earth-Sci. Rev., *46,* 167–185.

Anderson, L. 1979. Simultaneous spectrophotometric determination of nitrite and nitrate by flow injection analysis. Anal. Chim. Acta, *110,* 123–128.

Anschutz, P., C. Hyacinthe, P. Carbonel, J. M. Jouanneau and F. J. Jorissen. 1999. La distribution du phosphore inorganique dans les sédiments modernes du Golfe de Gascogne. C. R. Acad. Sci. Paris, *328,* 765–771.

Anschutz, P., B. Sundby, L. LeFrançois, G. W. Luther III and A. Mucci. 2000. Interaction between metal oxides and the species of nitrogen and iodine in bioturbated marine sediments. Geochim. Cosmochim. Acta, *64,* 2751–2763.

Anschutz, P., S. Zhong, B. Sundby, A. Mucci and C. Gobeil. 1998. Burial efficiency of phosphorus and the geochemistry of iron in continental margin sediments. Limnol. Oceanogr., *43,* 53–64.

Berner, R. A. 1980. Early diagenesis: A Theoretical Approach. Princeton University Press, Princeton, NJ, 241 pp.

Bernhard, J. M. 1988. Postmortem vital staining in benthic foraminifera: Duration and importance in population and distributional studies. J. Foram. Res., *18,* 143–46.

—— 1992. Benthic foraminiferal distribution and biomass related to porewater oxygen content: Central California continental slope and rise. Deep-Sea Res., *39,* 585–605.

—— 2000. Distinguishing live from dead foraminifera: methods review and proper applications. Micropaleontology, *46,* (Suppl. 1), 38–46.

Boudreau, B. P. 1996. The diffusive tortuosity of fine-grained unlithified sediments. Geochim. Cosmochim. Acta, *60,* 3139–3142.

—— 1997. Diagenetic Models and Their Implementation. Springer, Berlin, 414 pp.

Bouma, A. H. 1962. Sedimentology of Some Flysch Deposits: A Graphic Approach to Facies Interpretation. Elsevier, Amsterdam, 168 pp.

Buckley, D. E. and R. E. Cranston. 1988. Early diagenesis in deep sea turbidities: the imprint of paleo-oxidation zones. Geochim. Cosmochim. Acta, *52,* 2925–2939.

Corliss, B. H. and S. Emerson. 1990. Distribution of Rose Bengal stained deep-sea benthic foraminifera from the Nova Scotian continental margin and Gulf of Maine. Deep-Sea Res., *37,* 381–400.

Deflandre, B., A. Mucci, J.-P. Gagné, C. Guignard, B. Sundby and P. Anschutz. 2000. The 1996

flood event: disruption of the ongoing diagenesis of Saguenay fjord sediments. Proceedings of the fifty-third Canadian Geotechnical Conference, *1,* 117–122.

Deflandre, B., A. Mucci, J.-P. Gagné, C. Guignard, and B. Sundby. 2002. Early diagenetic processes in coastal marine sediments disturbed by a catastrophic sedimentation event, Geochim. Cosmochim. Acta, *66,* 2547–2558.

DeLange, G. J. 1986. Early diagenetic reaction in interbedded pelagic and turbiditic sediments in the Nares Abyssal Plain (Western North Atlantic): Consequences for the composition of sediment and interstitial water. Geochim. Cosmochim. Acta, *50,* 2543–2561.

Douglas, R. G., J. Liestman, C. Walch *et al.* 1980. The transition from live to sediment assemblage in benthic foraminifera from the southern California borderland, *in* Quaternary Depositional Environments from the Pacific Coast, M. E. Field, A. H. Bouma, I. P. Colburn *et al.,* eds., Society of Economic Paleontologists and Mineralogists, Los Angeles, 257–280.

Douglas, R. G., L. Wall and M. L. Cotton. 1978. The influence of sample quality and methods on the recovery of live benthic foraminifera in the southern California Bight. Bureau of Land Management, Technical report 20.0, *2,* Washington D.C., 1–37.

Fenchel, T. and B. J. Finlay. 1995. Ecology and Evolution in Anoxic Worlds, Oxford University Press, 276 pp.

Ferdelman, T. G. 1988. The distribution of sulfur, iron, manganese, copper and uranium in salt marsh sediment cores as determined by sequential extraction methods. M.Sc. thesis, University of Delaware, USA.

Fontanier, C., F. J. Jorissen, L. Licari, A. Alexandre, P. Anschutz and P. Carbonel. 2002. Live benthic foraminiferal faunas from the Bay of Biscay: Faunal density, composition, and microhabitats. Deep Sea Res. I, *49,* 751–785.

Gooday, A. J., L. A. Levin, P. Linke and T. Heeger. 1992. The role of benthic foraminifera in deep-sea food webs and carbon cycling *in* Deep-Sea Food Chains and the Global Carbon Cycle, G. T. Rowe and V. Patiente, eds., 63–91, Kluwer Academic Publishers.

Hall, P. O. J. and R. C. Aller. 1992. Rapid, small-volume flow injection analysis for ΣCO2 and NH4+ in marine and freshwaters. Limnol. Oceanogr., *37,* 1113–1119.

Helder, W. and J. F. Bakker. 1985. Shipboard comparison of micro- and mini electrodes for measuring oxygen distribution in marine sediments. Limnol. Oceanogr., *30,* 1106–1109.

Hess, S. and W. Kuhnt. 1996. Deep-sea benthic foraminiferal recolonization of the 1991 Mt. Pinatubo ash layer in the South China Sea. Mar. Micropal., *28,* 171–197.

Hulth, S., R. C. Aller and F. Gilbert. 1999. Coupled anoxic nitrification/manganese reduction in marine sediments. Geochim. Cosmochim. Acta, *63,* 49–66.

Hyacinthe, C., P. Anschutz, P. Carbonel, J. M. Jouanneau and F. J. Jorissen. 2001. Early diagenetic processes in the muddy sediments of the Bay of Biscay. Mar. Geol., *177,* 111–128.

Jorissen, F. J., M. A. Buzas, S. J. Culver and S. A. Kuehl. 1994. Vertical distribution of living benthic foraminifera in submarine canyons off New Jersey. J. Foram. Res., *24,* 28–36.

Jorissen, F. J., H. C. De Stigter and J. G. V. Widmark. 1995. A conceptual model explaining benthic foraminiferal microhabitats. Mar. Micropal., *26,* 3–15.

Kostka, J. E. and G. W. Luther III. 1994. Partitioning and speciation of solid phase iron in saltmarsh sediments. Geochim. Cosmochim. Acta, *58,* 1701–1710.

Li, Y. H. and S. Gregory. 1974. Diffusion of ions in seawater and in deep-sea sediments. Geochim. Cosmochim. Acta, *38,* 703–714.

Luther, III G. W., B. Sundby, G. L. Lewis, P. J. Brendel and N. Silverberg. 1997. Interactions of manganese with the nitrogen cycle: alternative pathways for dinitrogen formation. Geochim. Cosmochim. Acta, *61,* 4043–4052.

Lutze, G. F. and A. Altenbach. 1991. Technique for staining living benthic foraminifera with Rose Bengal. Geol. Jahrbuch, *A 128,* 251–265.

Middelburg, J. J., G. J. de Lange and C. H. Van der Weijden. 1987. Manganese solubility control in marine pore waters. Geochim. Cosmochim. Acta, *51,* 759–763.

Mucci, A. and H. M. Edenborn. 1992. Influence of an organic-poor landslide deposit on the early diagenesis of iron and manganese in a coastal marine sediment. Geochim. Cosmochim. Acta, *56,* 3909–3921.

Mucci, A., B. Sundby, M. Gehlen, T. Arakaki and N. Silverberg. 1999. The fate of carbon in continental shelf sediments: A case study. Deep Sea Res. II, *47,* 733–760.

Mulder T. and P. Cochonat. 1996. Classification of offshore mass movements. J. Sediment Res., *66,* 43–57.

Mulder, T., O. Weber, P. Anschutz, F. J. Jorissen and J. M. Jouanneau. 2001. A few months-old storm-generated turbidite deposited in the Capbreton Canyon (Bay of Biscay, S-W France). Geo. Mar. Lett., *21,* 149–156.

Myers, C. R. and K. H. Nealson. 1988. Microbial reduction of manganese oxides: interactions with iron and sulfur. Geochim. Cosmochim. Acta *52,* 2727–2732.

Nesteroff, W. D., S. Duplaix, J. Sauvage, Y. Lancelot, F. Melières and E. Vincent. 1968. Les dépôts récents du canyon de Cap-Breton. Bull. Soc. Géol. Fra., *10,* 218–252.

Ogawa, N. and P. Tauzin. 1973. Contribution à l'étude hydrologique et géochimique du Gouf de Capbreton. Bull. Inst. Géol. Bassin Aquitaine, *14,* 19–46.

Postma, D. 1985. Concentration of Mn and separation from Fe in sediments—I. Kinetics and stoichiometry of the reaction between birnessite and dissolved Fe(II) at 10°C. Geochim. Cosmochim. Acta *49,* 1023–1033.

Revsbech, N. P. 1983. In-situ measurements of oxygen profiles of sediments by use of oxygen microelectrodes, *in* Polarographic Oxygen Sensors, G. Forstner, ed., Springer-Verlag, Berlin, 265–273.

Revsbech, N. P. and B. B. Jørgensen. 1986. Microelectrodes: their use in microbial ecology, *in* Advances in Microbial Ecology, *9,* Plenum Press, NY, 293–352.

Sen Gupta, B. K., R. L. Lee and M. S. III May. 1981. Upwelling and an unusual assemblage of benthic foraminifera on the northern Florida continental slope. J. Paleontol., *55,* 853–857.

Shanmugam, G. 1997. The Bouma sequence and the turbidite mind set. Earth Sci. Rev., *42,* 201–229.

Stookey, L. L. 1970. Ferrozine—A new spectrophotometric reagent for iron. Anal. Chem. *42,* 779–781.

Strickland, J. D. H. and T. R. Parsons. 1972. A practical handbook of seawater analysis. Bull. Fish. Resour. Board Can., *167,* 1–311.

Thomson, J., I. Jarvis, D. R. H. Green, D. A. Green and T. Clayton. 1998. Mobility and immobility of redox-sensitive elements in deep-sea turbidites during shallow burial. Geochim. Cosmochim. Acta, *62,* 643–656.

Wilson, T. R. S., J. Thompson, S. Colley, D. J. Hydes and N. C. Higgs. 1985. Early organic diagenesis: Significance of progressive subsurface oxidation fronts in pelagic sediments. Geochim. Cosmochim. Acta, *49,* 811–822.

Received: *11 October, 2001;* revised: *19 November, 2002.*